

Green Self-Assembling Porphyrins and Chlorins as Mimics of the Natural Bacteriochlorophylls *c*, *d*, and *e*

Teodor Silviu Balaban,^{*[a]} Myriam Linke-Schaetzel,^[a] Anil Dnyanoba Bhise,^[a]
Nicolas Vanthuyne,^[b] and Christian Roussel^[b]

Keywords: Self-assembly / Bacteriochlorophyll / Porphyrinoids / Light-harvesting / J-aggregates / Circular dichroism / Chlorosome

Novel porphyrins and chlorins that self-assemble in nonpolar solvents in a manner similar to that of the bacteriochlorophylls *c*, *d*, and *e* have been synthesized by a common protective group approach. The supramolecular assemblies have broad and red-shifted absorption spectra in comparison to those of the monomeric building blocks. The presence of a carbonyl group in conjugation with the tetrapyrrolic macrocycle produces green colors both in the free bases and in their zinc complexes, which, after self-assembly, are thus perfect artificial mimics of the chlorosomal antennas encountered in green photosynthetic bacteria. Enantiopure building blocks produce large helical aggregates with *M* or *P* helicity determined by the chirality of the 1-hydroxyethyl substituent. It is demonstrated that the groups essential for self-or-

ganization to occur – namely the hydroxy group, the zinc metal atom and the carbonyl group – do not have to be collinear, as has been presumed until now. Surprisingly, the chlorin derivative does not show hyperchromicity relative to similarly substituted porphyrins. This fact allows us to conclude that the more readily available porphyrins may be used for efficient artificial antennas of potential use in solar devices; otherwise it is necessary to increase the number of synthetic steps in order to incorporate into chlorins the annulated cyclopentanone ring, a structural feature carefully optimized by evolution in all (bacterio)chlorophylls.

(© Wiley-VCH Verlag GmbH & Co. KGaA, 69451 Weinheim, Germany, 2004)

Introduction

The ubiquitous green color of light-harvesting apparatus is encountered in (bacterio)chlorophyll-based photosynthetic organisms. In conjunction with other pigments, such as carotenoids, the light absorption characteristics, which include broad wavelength ranges and high extinction coefficients, have been optimized during evolution in order to ensure conversion of light into biochemical energy by adaptation to different habitats. Thus, bacteria that live under the water surface at depths of over 50 m have evolved antenna systems different to those of bacteria or algae living at the surface, and these differ in turn from terrestrial plants in their light-harvesting systems. While the last, more highly evolved, of these species have developed protein complexes to bind chromophores, in the early green photosynthetic bacteria, due to the pressures of synthetic and genetic economy, self-assembly of bacteriochlorophylls *c*, *d*, and *e* (Figure 1) is used.^[1,2] This much simpler architectural construct, which is fully functional, is worth mimicking

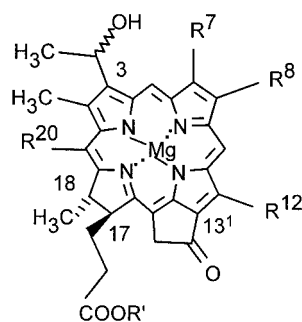
with robust and easily available pigments, for the goal of artificial photosynthesis.

Through the use of different spectroscopic techniques, we^[3] and others^[4] were involved fairly early on in the investigation of this intriguing self-assembly, although in the absence of definite crystallographic proof, structural details are still a matter of debate. Essential for the self-assembly algorithm to operate correctly are: (i) the 3-(1-hydroxyethyl) group (which may have either *R* or *S* stereochemistry), (ii) the 13¹-carbonyl group in the annulated five-membered ring, (iii) the central magnesium atom (although this may be replaced by other divalent diamagnetic metal ions such as zinc or cadmium), and (iv) the π – π interactions between the conjugated macrocycles. The close but ordered interaction between the chromophoric systems gives rise to broadened and red-shifted absorption maxima, which are beneficial for light-harvesting and, forms strongly fluorescent aggregates which can pass on the radiant energy to a trap from where the reaction center can be triggered for charge separation. The fluorescence quantum yields usually encountered with highly aggregated pigments are only very low, due to concentration quenching, a fact that hampers their use as photosensitizers in photovoltaic cells.

Here we present novel, fully synthetic pigments – namely a zinc porphyrin **10-Zn** and a zinc-chlorin **11-Zn** – capable

^[a] Forschungszentrum Karlsruhe, Institute for Nanotechnology, Postfach 3640, 76021 Karlsruhe, Germany
Fax: (internat.) + 49-(0)724-782-8298
E-mail: silviu.balaban@int.fzk.de

^[b] Université Aix-Marseille III, UMR: Chirotechnologie: catalyse et biocatalyse, Centre de Saint Jerome, 13397, Marseille, Cedex 20, France



R' = long chain: stearyl, cetyl,
oleyl, geranyl or farnesyl

R⁸ = CH₃, C₂H₅, *n*-C₃H₇, *s*-C₄H₉

R¹² = CH₃, C₂H₅

BChl c: R⁷ = R²⁰ = CH₃

BChl d: R⁷ = CH₃; R²⁰ = H

BChl e: R⁷ = CHO; R²⁰ = CH₃

Figure 1. Self-assembling bacteriochlorophylls encountered in the light-harvesting organelles known as chlorosomes (green sacs) of green photosynthetic bacteria

of self-assembly in similar manner to the bacteriochlorophylls *c*, *d*, and *e* possessing the same functional characteristics (*i-iv*). In a preliminary communication we described the structurally very similar porphyrins **12-Zn**–**16-Zn** (Figure 2), which were recently synthesized in our group and showed intense fluorescence after self-assembly.^[5] Furthermore, these could also be induced to self-assemble onto nanocrystalline titania.^[5,6] These were the first fully synthetic pigments capable of self-assembly similarly to that displayed by the natural (chlorosomal) bacteriochlorophylls. Tamiaki and co-workers had previously synthesized several self-assembling mimics, but these, being derived either from chlorophyll *a* or from bacteriochlorophyll *a*, are products of semisyntheses and thus involved rather tedious isolation and purification steps.^[7] Since our initial report,^[5] Tamiaki's group, using an elegant synthesis, have implemented the same design principles to obtain the self-assembling octaethylporphyrin-derived porphyrin **17-Zn**.^[8] The authors rightly argue that **17-Zn**, possessing only alkyl substituents, is more closely related than the *meso*-aryl-substituted porphyrins **12-Zn**–**16-Zn** to the natural BChls. If practical applications are envisaged,^[9] however, our compounds require fewer synthetic steps and so are more easily available, although octaethylporphyrin is a commercially available compound. As judged from the broad, red-shifted absorption spectra, structurally very similar self-assembly patterns were obtained from **12-Zn**, **13-Zn**, **14-Zn**, and **17-Zn**.^[5,8] These four compounds each have the hydroxy group

(originating either from an achiral hydroxymethyl or from a 1-hydroxyethyl group), the zinc atom, and the carbonyl group arranged collinearly. A very intriguing result is that the isomeric zinc porphyrin **18-Zn** failed to give red-shifted and broad absorption spectra upon self-assembly, which led the authors to speculate that collinearity of these three groups is an essential condition for the self-assembly to occur.^[8] As this observation was at odds with the fact that both **15-Zn** and **16-Zn** could self-assemble, we have now prepared **10-Zn**, with an angular disposition of these groups. We observed that it is the amount of π -overlap of the macrocycles in the self-assembled species that is responsible for the broadening and the red-shift of the absorption maxima, so the collinearity mentioned above is not a *sine qua non* for induction of self-organization.

Furthermore, we have now also synthesized the chlorin **11-Zn**, which because of its reduced symmetry was expected to display more intense Q-absorption bands than porphyrins, in a quest for an optimum self-assembling chromophoric system for hybrid solar cells.^[6] These are mixed organic-inorganic solar cells in which an antenna system additionally assures a large photon capture cross section for improved light-to-current conversion efficiencies under low light illumination conditions.

Results and Discussion

Syntheses: Scheme 1 presents the synthetic transformations, starting from the known copper porphyrin **1**^[10] with two *meso* 3,5-di-*tert*-butylphenyl groups^[11] and making use of 2,2-dimethyl-1,3-propanediol to protect *meso*-formyl groups, to enable the reduction both of a 3-acetyl group and of the porphyrin to the chlorin. While the isolated intermediates in the synthetic sequence of **10-Zn** are represented by even numbers, odd numbers are used for intermediates in the reaction steps leading to chlorin **11-Zn**. Monoformylation of **1** gave **2**, which was subsequently acetylated in a novel Friedel–Crafts type of acylation. After demetallation, the more reactive aldehyde group in **4** was protected in order to allow selective monoreduction of the acetyl group. Removal of the protective group and final zinc remetallation afforded **10-Zn** in a remarkable global yield of 43% over eight steps. For the synthesis of chlorin **11-Zn**, diformylation of **1** was performed, followed by double protection of the two *meso*-formyl groups in order to permit selective reduction of the porphyrin to the chlorin. Again, removal of the protective groups (*vide infra*) and final zinc metallation provided the desired chlorin **11-Zn**, albeit in a much lower global yield due to the simultaneous transformations in both the northern and southern part of the macrocycle.

Like our previous porphyrins **12**–**16-Zn**^[5] and Tamiaki's octaethylporphyrin-based compound **17-Zn**,^[8] **10-Zn** and **11-Zn** are fully synthetic mimics of the natural bacteriochlorophylls and are capable of self-assembly. Our synthetic concept is to use preformed porphyrins, which are available in multigram quantities, and, by means of selective trans-

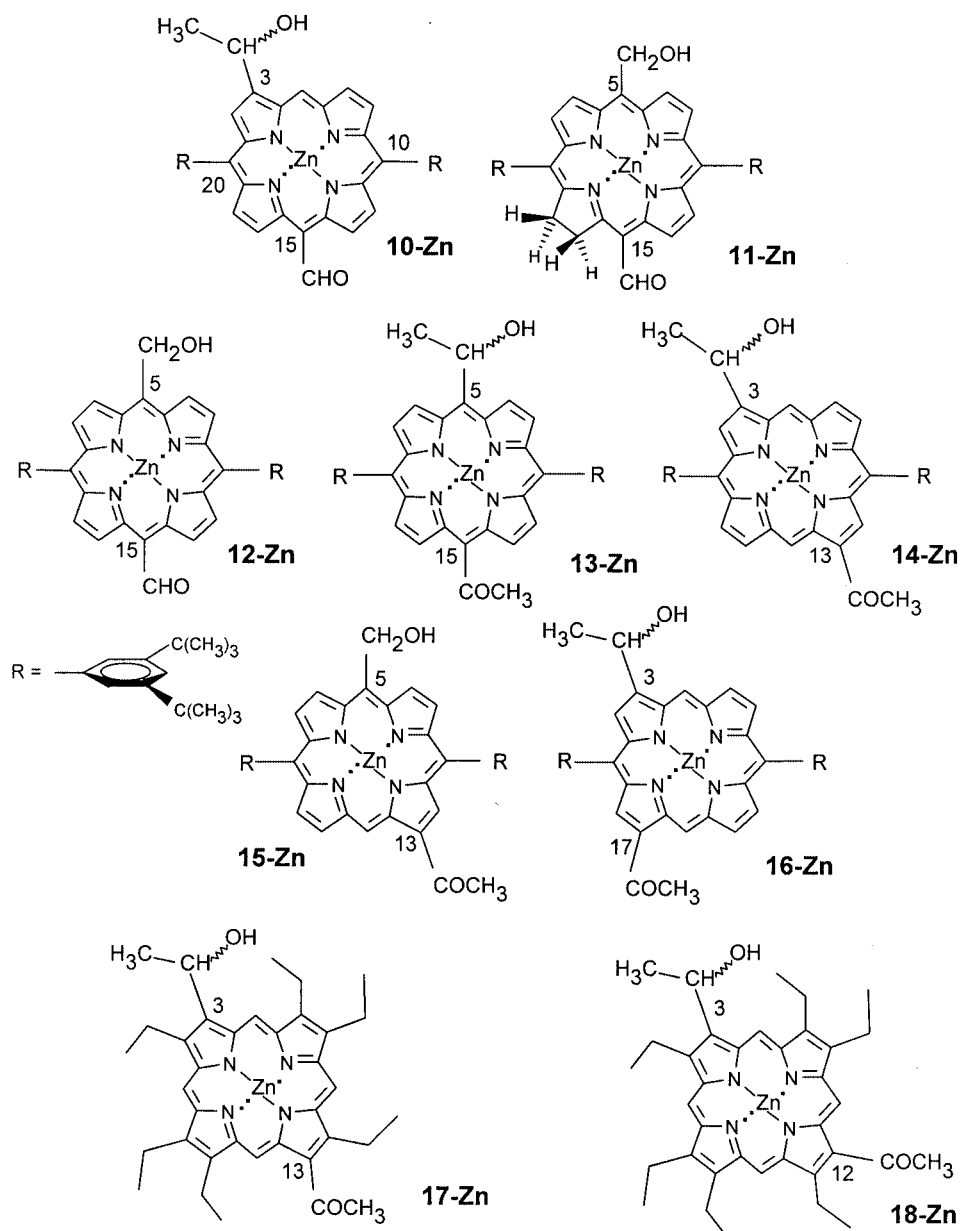
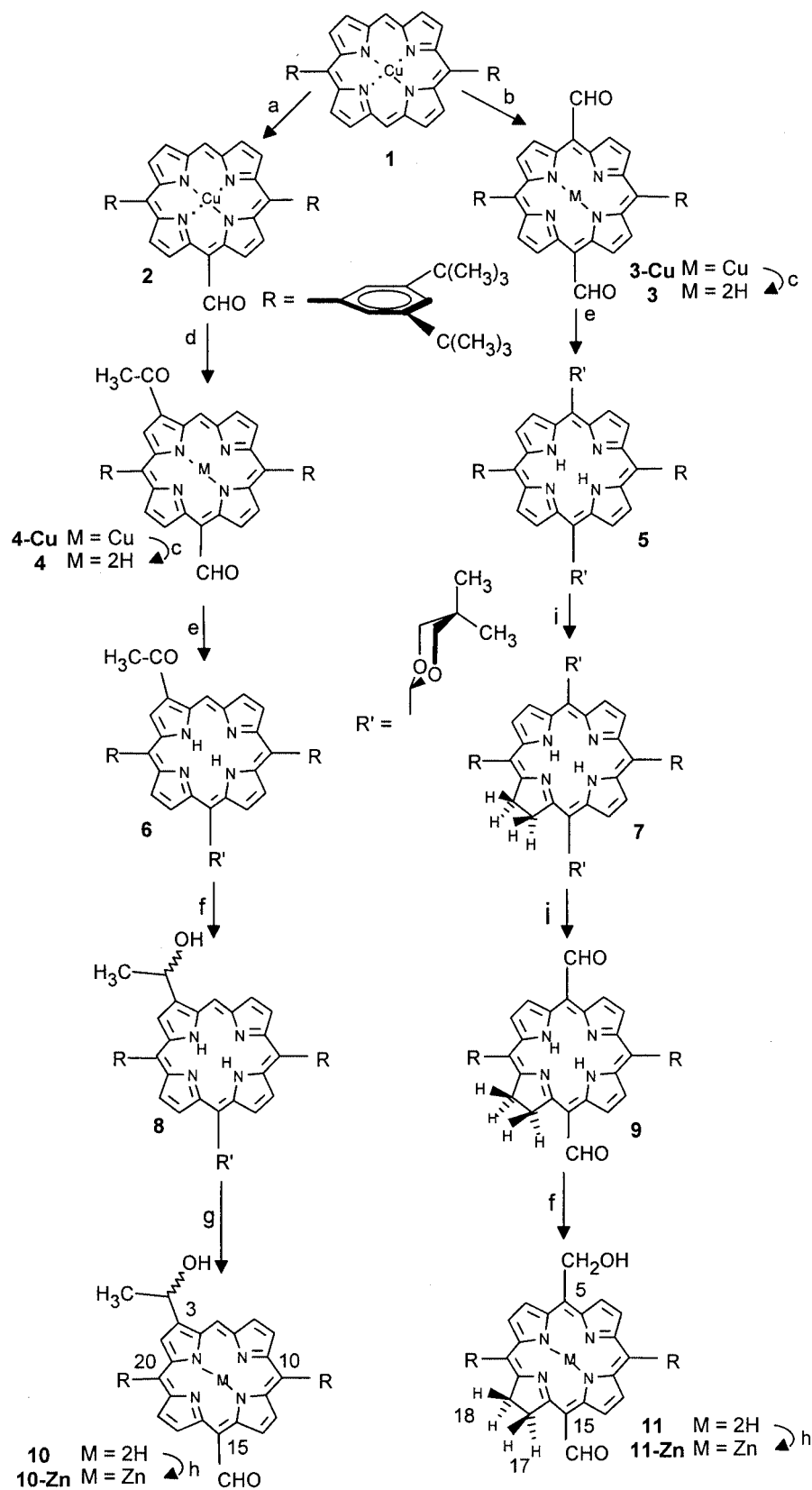


Figure 2. Synthetic mimics of the self-assembling BChls *c*, *d*, and *e*

formations, to equip these with groups programming a self-assembly algorithm.^[12] The final structure, and its properties are encoded in the architecture of the monomeric building block, or tecton.^[13]

Figure 3 shows the NMR spectra for the monomeric methanol adducts of the novel **10-Zn** porphyrin in comparison with the isomeric compound **15-Zn**, which nicely reflect the structural differences between the two isomers. It is interesting to note that the aromatic signals of the two nonequivalent 3,5-di-*tert*-butylphenyl groups appear well separated at 300 MHz in the case of **15-Zn** but are almost superimposed for **Zn-10**. This is probably due to the influence of the carbonyl group, which makes the *meso*-aryl groups differ more when it is present in the 13-position (as an acetyl group) in **Zn-15** than when it is present in the 15-*meso*-position (as a formyl group) in **Zn-10**.

Natural chlorins have been shown to photosensitize nanocrystalline titania effectively,^[14] and Lindsey's group has recently developed rational synthetic routes to chlorins.^[15] We have applied the protective group strategy shown in Scheme 1 to allow reduction of the porphyrin followed by unmasking of the now nonequivalent formyl groups. Several protecting strategies were tried [bis(*m*)ethyl acetals or 1,3-dioxolane], but only the *gem*-dimethyl-substituted dioxane group, also introduced to porphyrin chemistry by Lindsey,^[16] gave satisfactory results. The porphyrin reduction works smoothly with tosylhydrazide^[17] for all protective groups tried, but the deprotection step requires gentle conditions under which only the Lindsey 1,3-dioxane is cleaved properly. In this case we were able to suppress the competing "decarbonylation" reaction in which the formyl protected group is replaced by a *meso*-hydrogen atom. This ser-



Scheme 1. Reagents and conditions: *a*: POCl_3/DMF , $\text{ClCH}_2\text{CH}_2\text{Cl}$, 40°C , 45 min, 83%;^[5] *b*: POCl_3/DMF , $\text{ClCH}_2\text{CH}_2\text{Cl}$, 60°C , 14 h, 43%;^[5] *c*: $\text{TFA}/\text{H}_2\text{SO}_4$ (1:1 v/v), >85%;^[5] *d*: Ac_2O , $\text{SnCl}_4/\text{CS}_2$, 0°C , 3 min, 80% (after demetallation as in *c*);^[5] *e*: 2,2-dimethyl-1,3-propanediol, PTSA , toluene, Δ , 65 min – 6 h, 75–96%; *f*: NaBH_4 , MeOH , CH_2Cl_2 , room temp., 0.5–19 h, 50–72%; *g*: HCl , 1,4-dioxane, Ar, room temp., 17 h, 94%; *h*: $\text{Zn}(\text{OAc})_2$, $\text{CHCl}_3/\text{MeOH}$ (5:3, v/v), room temp., 3 h, 93–95%; *i*: Ts-NH-NH_2 , K_2CO_3 , β -picoline, Δ , 15 h, 55%; *j*: TiCl_4 , CHCl_3 , room temp., 15 min, 66%.

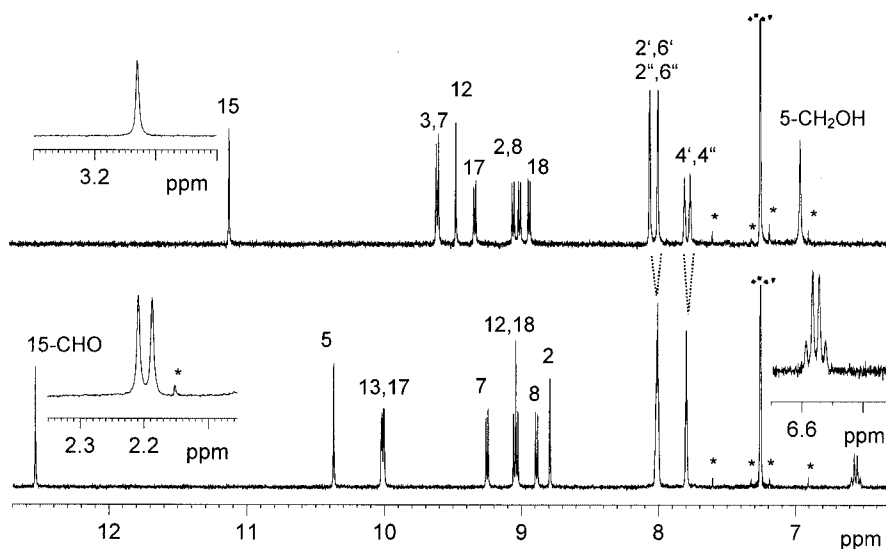


Figure 3. Low-field region of the 300 MHz NMR spectra of **10-Zn** (lower trace) and **15-Zn** (upper trace) in $\text{CDCl}_3:\text{CD}_3\text{OD}$ 10:1 (v/v). Assignments are based on COSY and NOESY spectra; insets show the 3- CHOHCH_3 signals (lower trace) and the 13- COCH_3 singlet (upper trace); the peaks indicated by asterisks do not belong to the sample, being either ^{13}C -satellites and spinning side bands of the CHCl_3 signal or a trace of acetone.

endipitously found reaction sequence might prove to be of some synthetic interest for selective removal of *meso*-substituted formyl groups, but this was not in our interest in the current study.

Remarkable in our case is the potential to reduce the 5-formyl group in **9** selectively, leaving the 15-formyl group in the 17,18-dihydroporphyrin intact.^[18] With excess reagent and prolonged reaction times, the 15-formyl group starts to become reduced. We were not able to separate the other isomeric formyl-hydroxymethylene-chlorin isomer cleanly from these reaction mixtures as the dihydroxymethylene compound is also formed concomitantly. As in the case of the related dicarbonyl porphyrins,^[5] it is interesting to note that the possibility of isolating the monoreduced hydroxyoxo compounds in relatively high yields is due to the fact that one carbonyl group activates the other. In the case of symmetrical compounds (i.e., equivalent carbonyl groups), after the reduction of the first CO group, the second is reduced much more sluggishly, accounting for this unexpected product selectivity. With nonequivalent CO groups, as is the case in **9**, the less sterically hindered one (i.e., the 5-CHO group) is reduced more rapidly.

An unhindered *meso*-carbonyl group is not only more reactive but also produces a green color not only in chlorins but even in the free base porphyrins.^[19] It is thus interesting to note that while a *meso*-formyl group situated in the porphyrin plane gives green colored free base porphyrins, a *meso*-acetyl group is forced out of conjugation with the macrocycle, due to buttressing of the methyl group by the β -pyrrolic protons. This translates into a hypsochromic shift, resulting in the “normal”, purple colored free base and zinc metalated porphyrins such as **13-Zn**.^[5] An acetyl group in an unhindered β -pyrrolic position, however, can adopt planar conformations and thus again give rise to green colored compounds such as **14-Zn**, **15-Zn**, or **16-Zn**. In the

LH2 and LH3 light-harvesting complexes of purple bacteria, which have been characterized by X-ray crystallography,^[20,21] conjugation of an acetyl group in a β -pyrrolic position in a chlorin ring (in bacteriochlorophyll *a*) can be finely tuned by the protein matrix. This shifts the absorption spectrum from 850 nm for the B850 ring in LH2 to 820 nm in LH3, just through titling of the acetyl group out of conjugation (dihedral angles of 15° in LH2 and 43° in LH3). This has profound implications for the light-harvesting ability of these bacteria, which produce LH3 complexes only under low light illumination conditions.

UV/Vis Absorption Properties of the Assemblies: That self-assembly is fully operational in **10-Zn** can be seen in nonpolar solvents by the broad and red-shifted absorption maxima of both the Soret and Q bands (Figure 4, part A) and by the strong Rayleigh light scattering. Also presented here for the first time, for comparison, are the corresponding absorption spectra of the isomeric compound **15-Zn** (Figure 4, part B). This allows direct comparison between the achiral hydroxymethylene group and the hydroxyethyl group as ligands for the zinc atoms in the self-assembled structures. Complete disassembly is ensured by addition of minute (but suprastoichiometric) amounts of a competing solvent, such as methanol, for Zn-ligation, which is also expected to disrupt any intermolecular hydrogen bonding (Figure 4, dotted traces). It is evident from the spectra that almost no monomeric **15-Zn** (shoulder at 405 nm) is present, whereas for **10-Zn** there are considerable amounts of monomers present (sharp Soret band at 420 nm), in addition to self-assembled species characterized by the broad and red-shifted absorptions. Three bands are diagnostic for the self-assembly, one corresponding to the Soret band and two smaller ones corresponding to the Q_x and Q_y bands and indicated by arrows in Figure 4. Titration of MeOH indicates that a monomeric Zn–MeOH adduct is formed,

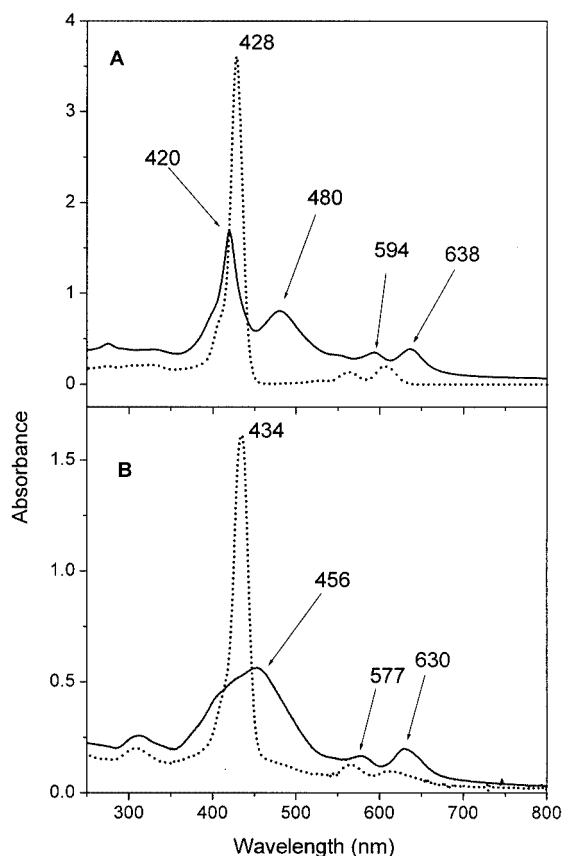


Figure 4. Self-assembled **10-Zn** (50 μM , part **A**) and **15-Zn** (11 μM , part **B**) in dry *n*-heptane at room temperature (full traces); the dotted traces are for the same samples after addition of supra-stoichiometric amounts of methanol; path-length was 0.5 cm for all traces; for the **10-Zn**-MeOH adduct (part **A**, dotted trace) the solution was diluted with an equal volume of *n*-heptane

its Soret band being slightly red-shifted by ≈ 8 nm in relation to the non-ligated monomers. It is, however, instructive to compare the wavelength difference between the aggregate bands and those of these methanol adducts: $\Delta\lambda_{\text{max.}} = 52$ nm and 22 nm for the corresponding Soret bands of **10-Zn** and **15-Zn**, respectively. The two Q bands have different intensities because of the different transition probabilities in these two desymmetrized porphyrins. Interestingly, in the self-assembled species, the most strongly red-shifted Q band is also the more intense one, as in the **10-Zn**-MeOH adduct. In **15-Zn** the red-shifted aggregate band at 630 nm is also more intense, but a reversal occurs for the **15-Zn**-MeOH adduct. This implies a $\Delta\lambda_{\text{max.}} = 75$ nm for this transition, which allows us to conclude that very similar self-assembled structures are actually obtained in both cases, giving rise to red-shifted spectra as for J-aggregates.^[22] The anchoring group is hydroxy(m)ethyl, which binds a zinc atom of a neighboring porphyrin, while the direction of the Q_y transition is determined by the carbonyl group, which must thus have slightly different relative orientations in the two supramolecules, as indicated by the

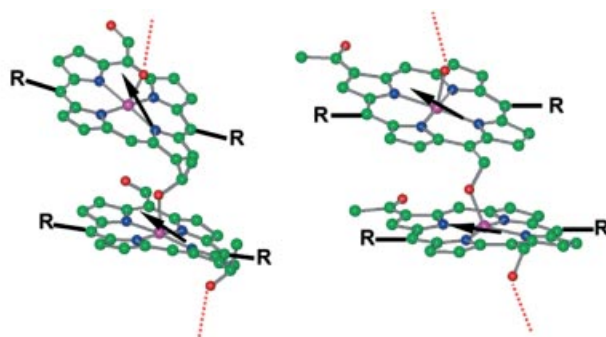


Figure 5. Stacking interactions in **10-Zn** (left) and **15-Zn** (right); R = 3,5-di-*tert*-butylphenyl; only two porphyrin rings are shown in each case, together with the directions of the Q_y transition dipole moments (arrows); the geometries were obtained by successive optimizations with the semiempirical force-field PM3 and molecular mechanics (MM+) by use of the HyperChem[®] [23] program package and should be regarded only as a crude approximation

molecular models shown in Figure 5. Subtle variations in the π -overlap and/or optical properties of the assemblies can be engineered by varying the positions of attachment to the porphyrin macrocycle of the anchoring and carbonyl groups. We can rule out formation of closed dimers by double coordination of the zinc atoms by the hydroxy-(m)ethyl groups, which would also lead to parallel but opposing Q_y transition dipole moments and should thus be blue-shifted. More probably, the large assemblies are formed of extended stacks of different lengths, as implied by the dotted lines in Figure 5. The different lengths account for the heterogeneity and thus the broad absorption maxima.

The temperature dependence of the absorption spectra for **10-Zn** shows that gradual disassembly (vide supra) occurs upon heating (Figure 6). In heptane, even at 95 $^{\circ}\text{C}$, a considerable amount of aggregates still persist but their size has been trimmed as observed from the step-wise decrease in light scattering. Only relative large aggregates and small units, which could be, for instance, either monomers or dimers, seem to be present in equilibrium.

No quantitative description of the aggregation is yet possible, due to the uncertain size of the aggregates. We therefore limit ourselves here to a qualitative description, showing not only that the temperature decreases the aggregation tendency (cf. Figure 6), but also that the concentration plays an important role (inset in Figure 6); a critical nucleus must be formed so that aggregation proceeds; that is, more molecules can become part of the aggregate more rapidly than others are being disassembled.

The above examples clearly show that a linear arrangement of the zinc-chelating hydroxy group and the carbonyl group is not necessary for induction of the self-assembly algorithm. It is thus surprising that Tamiaki's compound **18-Zn** failed to show self-assembly. In our opinion sterical hindrance by interlocked ethyl groups cannot be invoked, as the isomeric compound **17-Zn** self-assembles readily. Rather, we suspect that the concentration range studied was too dilute for red-shifted absorption maxima to be detectable and that stack formation must also occur, although less

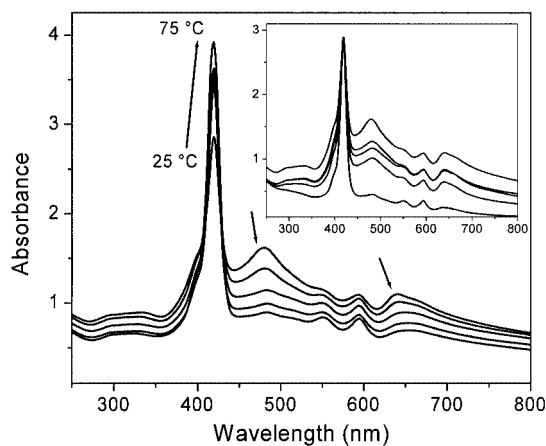


Figure 6. Variable temperature absorption spectra of self-assembled (*rac*)-**10-Zn** in *n*-heptane (70 μM); the 1-cm path-length cuvette was heated in 10° increments and the trace at 65 °C is not shown; note the gradual decrease in the scattering contribution, which usually produces a shift of the baseline; Inset – concentration dependence of the aggregation at 25 °C; traces have been scaled vertically at the Soret maximum of the monomer by multiplication with the following scaling factors (from the top trace to the bottom one): 1, 1.6, 2.3, 3.3, 13.2; the samples were prepared by dilution of a 3.7 mM CH_2Cl_2 solution of **10-Zn** with 2 mL dry *n*-heptane and had the following concentrations calculated for monomeric species: 70, 40, 30, 20, and 10 μM

readily, with **18-Zn**. In support of this hypothesis, here we present the absorption spectra for **16-Zn**, self-assembled at two different concentrations, and after disassembly with methanol (Figure 7). While the 478, 510, and 640 aggregate maxima are barely discernible in the more dilute samples, they are clearly evident at higher concentration. The content of monomers is much higher in **16-Zn**, however, and so, as with Tamiaki's compound **18-Zn**, self-assembly, although possible, is somewhat inhibited. The bulky 3,5-di-*tert*-butylphenyl groups present in our case are surely much more sterically demanding than the readily rotating ethyl sub-

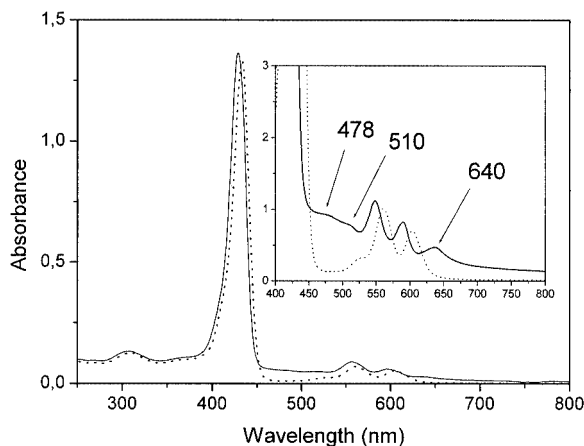


Figure 7. Absorption spectra of **Zn-16** under conditions similar to those of Figure 4 and 6, and with a path-length of 0.5 cm; dotted lines after disassembly with methanol; inset: a five times more concentrated sample (50 μM) exhibiting more self-assembled species, which give the red-shifted absorption maxima indicated by the arrows

stituents. This fact again supports the notion that the main interaction is the zinc coordination by the hydroxy substituent, and that this determines the amount of π -stacking interactions after interdigitation of the peripheral substituents. We are currently pursuing single-crystal growth and X-ray diffraction studies on several of our compounds, which hopefully will shed light on the details of the self-assembled architectures.^[24]

Figure 8 presents the absorption spectra of the chlorin **11-Zn**, both after self-assembly and as the monomeric methanol adduct. Similarly to the case of the porphyrin **10-Zn**, several broad, almost featureless bands (indicated by the arrows), are encountered for the self-assembled species. However, more transitions are clearly discernible. This is due to the more strongly desymmetrized chlorin and to considerable variations in the size of the aggregates, which result in inhomogeneous broadening. The broad Soret bands in the aggregates almost overlap with the Q_x bands in the monomers or dimers. A broad wavelength absorption range is advantageous, as it allows a larger portion of the solar spectrum to be used for light-harvesting.

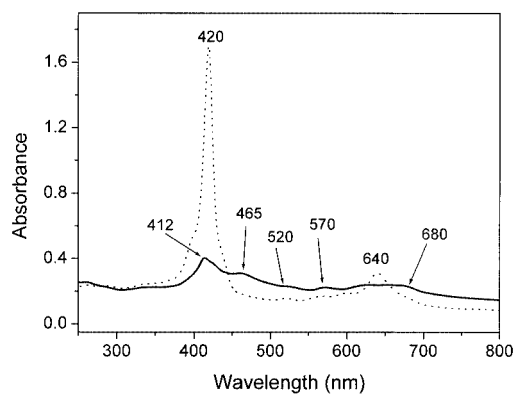


Figure 8. UV/Vis spectra of the self-assembled chlorin **Zn-11** in dry *n*-heptane. Dotted trace is after disassembly with methanol ($c = 17 \mu\text{M}$); both spectra were recorded at room temperature with a path-length of 1 cm

Another important observation can be made from the absorption spectra in Figure 4 and 8 on the basis of the extinction coefficients of the chlorin **11-Zn** in comparison to the porphyrins **10-Zn** either as the racemate or as separated enantiomers (*vide infra*). While for the Q band the $\log \epsilon$ value is practically the same (4.16 versus 4.19), the Soret band is markedly decreased, by a factor of almost 3, in the chlorin ($\log \epsilon = 5.01$) in relation to the porphyrin ($\log \epsilon = 5.47$). Contrary to expectations based on nonquantitative absorption data, simple self-assembling chlorins, although they do present broad absorptions, thus allowing a large wavelength palette of the solar spectrum to be harvested (Figure 8), should not be superior to porphyrins as artificial antenna systems. In (bacterio)chlorophylls, while the Soret band is as intense as in our chlorin ($\log \epsilon = 5.01$ in diethyl ether), the Q-band is markedly increased by a factor of 5.9 ($\log \epsilon = 4.93$ versus 4.16).^[25] It thus appears that the cyclopentanone moiety in the natural chlorophylls

is an important structural element carefully optimized by evolution. Although excellent synthetic methodologies for annulation of such oxo-five-membered rings to porphyrins and chlorins have been developed, these involve several additional synthetic steps.^[26] This structural element also forces the 13¹-carbonyl group into co-planarity with the tetrapyrrolic macrocycle.

CD-Spectroscopy and the Supramolecular Chirality of Self-Assembly: The separated enantiomers of the free base **10**, after zinc metallation and self-assembly, give helical superstructures which display giant (or PSI-type^[27]) circular dichroism (CD) with mirror imaged exciton couplets in the region of the red-shifted Soret aggregate band. From the positive or negative Cotton effect appearing at the longer wavelength, a clockwise or counterclockwise disposition of the transition dipole moments^[28] in the π -stacked porphyrins can be assigned to the assemblies formed from the enantiomers eluted first and second, respectively (Figure 9). Addition of polar solvents such as methanol again leads to disassembly, which is accompanied by the disappearance of the intense CD signals and a markedly increased, blue-shifted Soret absorption band (Figure 10).

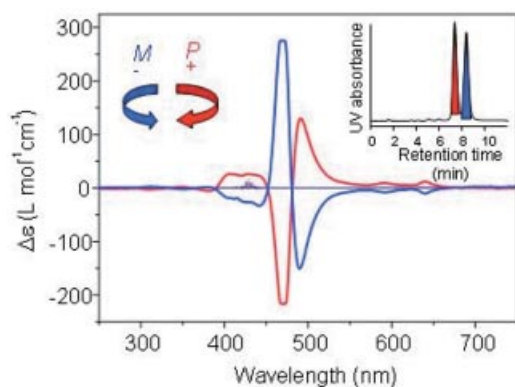


Figure 9. CD spectra of self-assembled **10-Zn**; red trace – first eluted enantiomer of **10** after metallation with zinc acetate and self-assembly in *n*-heptane (28 μ M solution); blue trace – second eluted enantiomer of **10** after Zn insertion and self-assembly in *n*-heptane (22 μ M solution); the strongest Cotton effects are slightly truncated due to saturation of the detector; in more dilute solutions the self-assembly was less pronounced, while with thinner cuvettes the Cotton effects of the Q-bands were less visible; dotted traces, superimposing the zero line, are after disassembly with methanol; in these cases practically no light passed through the sample at \approx 430 nm anymore, due to the intense Soret absorption of the monomers; the spectra were recorded at room temperature with a path length of 1 cm; the inset shows a typical preparative chiral HPLC trace (for details see the Exp. Sect.)

At present, we cannot tell whether the self-assembly process with *rac*-**10-Zn** occurs equally well between the separated *R* and *S* enantiomers or if a hetero-enantiomeric process is energetically preferred. However, it appears that the separated enantiomers are less prone to self-assembly than similarly treated racemate samples. We can rule out impurities leaking from the chiral HPLC column or traces of polar solvents inhibiting their aggregation, as these were subsequently removed in a further purification step. An experimental observation is that the size of the aggregates is

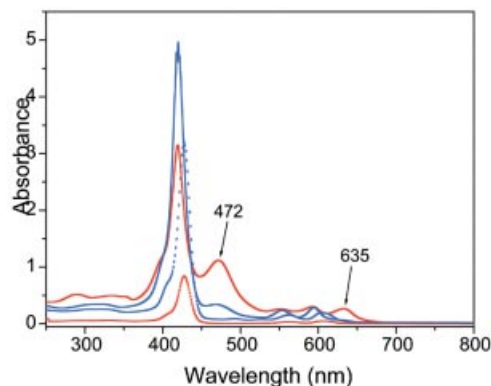


Figure 10. UV/Vis spectra of self-assembled **10-Zn**; red trace – first eluted enantiomer of **10** after metallation with zinc acetate and self-assembly in *n*-heptane (28 μ M solution); blue trace – second eluted enantiomer of **10** after Zn insertion and self-assembly in *n*-heptane (22 μ M solution); the red trace represents more self-assembled species with maxima at 472 and 635 nm than the blue trace; the spectra were recorded at room temperature with a path-length of 1 cm; dotted traces are after disassembly with methanol; the red dotted trace was recorded with a 0.1-cm path length, while the blue dotted trace was recorded with a 0.5-cm path length; note the much smaller ratio between the aggregate maxima and the bands of the monomers in comparison with the *rac*-**10-Zn**, shown in Figure 4, part A and in Figure 6

strongly dependent on the initial concentration of the monomers. It has also recently been shown,^[29] and theoretically explained,^[30] that the CD signals are also strongly dependent on the size of the aggregates, and even that sign reversals of the longest-wavelength Cotton effect may occur, simply with increasing length of tubular aggregates of chromophores.

From ongoing work in Tamiaki's group, which has assigned the stereochemistry of 3-hydroxyethyl groups attached to porphyrins, bacteriochlorophylls, and bacteriochlorins through correlation of NMR chemical shifts in Mosher-type esters,^[31] we tentatively assign the 3¹-*R* configuration to the enantiomer eluted first and the 3¹-*S* configuration to the enantiomer eluted second. Assuming that no strange size effects occur in the CD spectra, the first and the second eluted enantiomers produce *P*- and *M*-type helical suprastructures, respectively. In future work we will use complementary methods to verify this assignment.

Conclusion

We have extended the self-assembly algorithm which operates in the chlorosomes of photosynthetic bacteria to synthetic porphyrins and chlorins, thus establishing its generality. The separated enantiomers of **10-Zn** form chiral suprastructures displaying opposite chiralities after self-assembly. The "molecular" chirality of the hydroxyethyl group is thus transferred at the "supramolecular" level. Interestingly, the separated enantiomers appear to self-assemble less readily than the racemate at the same concentrations. This observation might explain why in the chlorosomes both enantiomers of the 3-hydroxyethyl group are present within various homologues.

Our novel self-assembling zinc porphyrins present attractive optical properties, which might make them useful in artificial light-harvesting devices. The presence of carbonyl groups in conjugation with the macrocycle produce a green color both in the free bases and in the zinc complexes, thus mimicking the natural antenna systems. Surprisingly, similar simple chlorins do not show higher extinction coefficients for the Q bands and have Soret bands of reduced intensity. If only the relative proportions are considered, then the Q bands in chlorins indeed appear to be more intense than those of the more symmetric porphyrins. In chlorophylls the annulated cyclopentanone ring has a special functional role in further desymmetrizing the macrocycle and at the same time it ensures a coplanar carbonyl group, fully conjugated with the macrocycle. Whether it is worth implementing this extra ring for artificial devices is a matter of device performance and ultimately cost. We would like to encourage studies in this area, stressing that for organic solar cells the cost-limiting factor is not the chemical synthesis of the components involved but rather the modest performance ($\approx 3\%$).^[32] A doubling of this value – through the use of artificial antennas as in natural light-harvesting, for instance – might prove an economically viable alternative to the currently still costly silicon-based solar cells, which can, however, attain $\approx 14\%$ energy conversion efficiencies in industrially produced devices.

Experimental Section

General Remarks: Solvents were dried and freshly distilled before use as follows: dichloromethane from calcium hydride; toluene and *n*-heptane from sodium metal; [D]chloroform from phosphorus pentoxide. NMR spectra were recorded at 300 MHz (¹H) with a Bruker DPX 300 Avance spectrometer. Chemical shifts are given in ppm relative to the signal of CHCl₃ which was taken as $\delta = 7.26$ (for ¹H) and 77.00 ppm (for ¹³C). Analytical chiral HPLC analyses of **10**, **13**, **14**, and **16** were performed on a screening unit composed of a Merck D-7000 system manager, Merck–Lachrom L-7100 pump, Merck–Lachrom L-7360 oven capable of accommodating 12 columns fed by a Valco 12 positions valve, and Merck–Lachrom L-7400 UV detector. Generally, the free bases were better resolved than the corresponding Zn complexes. Separation of **10** was obtained on a chiral (*S,S*)-Whelk–O1 (250 × 46 mm, Regis) column with *n*-hexane/ethanol (9:1, v/v) at 25 °C at 2 mL/min and with UV detection at 420 nm. Retention times were $R(t_1) = 7.36$ min and $R(t_2) = 8.36$ min; retention factors $k_1 = 3.91$ and $k_2 = 4.58$; selectivity factor $\alpha = k_2/k_1 = 1.17$ and resolution $R_s = 1.70$. Preparative chiral HPLC was performed on the same column under the same conditions with use of a Merck–Hitachi LiChrograph L-6000 pump, Merck–Hitachi L-4000 UV detector, and Merck D-7000 system manager. *n*-Hexane and ethanol were HPLC grade from SDS (Peypin, France). The solvents for the chromatography experiments were degassed and filtered through a Millipore membrane (0.45 μ m) before use. Further details of the chiral separations are included in the CHIRBASE[®] database.^[33] UV/Vis spectra were measured with a Varian Cary 500 instrument. The variable temperature spectra were performed with the aid of a Peltier heating unit allowing equilibration of temperature before each curve was measured while the solution in the quartz cuvette was stirred with a magnetic stirrer. MALDI-TOF mass spectra

were obtained on a Voyager Instrument from Applied Biosystems, with anhydrous glycerol, HABA [2'-(4-hydroxyphenylazo)benzoic acid], or 1,8,9-anthracenetriol matrices. HR-FAB-MS were recorded with 3-nitrobenzyl alcohol (NBA) as the matrix on a Finnigan MAT 90 machine. CD spectra were measured with an JASCO J-810 CD spectrometer with 2 s integration time and with a 2 nm bandwidth with baseline subtraction. The baseline was recorded with *n*-heptane alone in a cuvette identical to that used for recording the samples. Thin layer chromatography was performed on silica gel plates from Macherey–Nagel. Column chromatography was performed with Merck silica gel 40–63 μ m.

3-Acetyl-10,20-bis(3,5-di-*tert*-butylphenyl)-15-(5,5-dimethyl-1,3-dioxan-2-yl)porphyrin (6): (Transformation **e** in the Scheme). 3-Acetyl-10,20-bis(3,5-di-*tert*-butylphenyl)-15-formylporphyrin (**4**)^[5] (0.200 g, 0.26 mmol), neopentyl glycol (0.255 g, 2.44 mmol), *p*-toluenesulfonic acid (0.018 g, 0.094 mmol), and toluene (140 mL) were placed in a 250 mL flask fitted with a Dean–Stark trap and a reflux condenser, and the mixture was heated to reflux for 65 min. The reaction mixture was then cooled and was washed with a saturated NaHCO₃ solution and then with water. The organic layer was then dried with Na₂SO₄. After solvent evaporation, **6** was obtained as a purple solid (0.215 mg, 96%). ¹H NMR (300 MHz, CDCl₃): $\delta = 11.30$ (s, 1 H, 5-H), 10.10 (d, ³*J* = 4.8 Hz, 1 H, 13-H), 9.80 (d, ³*J* = 4.8 Hz, 1 H, 17-H), 9.45 (d, ³*J* = 4.8 Hz, 1 H, 7-H), 9.40 (s, 1 H, 2-H), 9.11 (d, ³*J* = 5.1 Hz, 1 H, 12-H), 9.01 (d, ³*J* = 4.5 Hz, 1 H, 18-H), 8.94 (d, ³*J* = 4.8 Hz, 1 H, 8-H), 8.10 (d, ⁴*J* = 1.8 Hz, 2 H, 2', 6'), 8.06 (d, ⁴*J* = 1.8 Hz, 2 H, 2'', 6''), 7.97 (s, 1 H, H_{acetal}), 7.87 (t, ⁴*J* = 1.5 Hz, 1 H, 4'), 7.83 (t, ⁴*J* = 1.8 Hz, 1 H, 4''), 4.33 (s, 4 H, CH₂ acetal), 3.13 (s, 3 H, COCH₃), 1.93 (s, 3 H, CH₃ eq-acetal), 1.12 (s, 3 H, CH₃ax-acetal), –2.83 (s, 2 H, NH) ppm. UV/Vis (CH₂Cl₂): λ_{max} (nm) = 428, 534, 576, 603, 661. HR-FAB-MS: found *m/z* = 843.5195 [M + H]⁺, calcd. for C₅₆H₆₇N₄O₃ 843.5213.

rac-10,20-Bis(3,5-di-*tert*-butylphenyl)-15-(5,5-dimethyl-1,3-dioxan-2-yl)-3-(hydroxyethyl)porphyrin (8): (Transformation **f** in the Scheme). Compound **6** (160 mg, 0.1897 mmol), NaBH₄ (143.5 mg, 0.379 mmol), methanol (12 mL), and dichloromethane (25 mL) were stirred in a 100 mL single-necked flask at room temp. for 19 h. The reaction mixture was then washed twice with brine and dried with Na₂SO₄, after which the solvents were evaporated to leave a crude product, which was then purified by column chromatography (SiO₂, eluted with CH₂Cl₂) to give pure purple compound **8** (115 mg, 72%). ¹H NMR (300 MHz, CDCl₃): $\delta = 10.42$ (s, 1 H, 5-H), 10.02 and 9.97 (two d, 2 H, ³*J* = 4.5 Hz, 13- and 17-H), 9.34 (d, ³*J* = 4.5 Hz, 1 H, 7-H), 9.03 (two partially overlapping d, 3 H, 12, 18 and 8-H), 8.91 (s, 1 H, 2-H), 8.09 and 8.08 (two d, ⁴*J* = 1.8 Hz, 4 H, 2', 6' and 2'', 6''-H), 8.03 (s, 1 H, 2-H_{acetal}), 7.84 (t, ⁴*J* = 1.8 Hz, 2 H, 4', 4''-H), 6.65 (quint, 1 H, HO–CH–CH₃), 4.34 (s, 4 H, CH₂-acetal), 2.59 (d, ³*J* = 4.5 Hz, 1 H, OH), 2.26 (d, ³*J* = 6.3 Hz, 3 H, 6.6 Hz, HO–CH–CH₃), 1.95 (s, 3 H, CH₃-eq-acetal), 1.57 (two s, 2 × 18 H, C(CH₃)₃), 1.13 (s, 3 H, CH₃-ax-acetal), –3.05 (s, 2 H, N–H) ppm. UV/Vis (CH₂Cl₂): λ_{max} (nm) = 414, 510, 573, and other two less intense Q bands. HR-FAB-MS: *m/z* = 845.5357 [M + H]⁺, calcd. for C₅₆H₆₉N₄O₃ 845.5370.

rac-10,20-Bis(3,5-di-*tert*-butylphenyl)-15-formyl-3-(1-hydroxyethyl)porphyrin (10): (Transformation **g** in the Scheme). Aqueous HCl (20 mL, 0.5 M) was added to a solution of compound **8** (100 mg, 0.118 mmol) in 1,4-dioxane (30 mL) under inert atmosphere, and the mixture was stirred at room temp. for 17 h. After completion of the reaction (TLC monitoring), the mixture was washed with brine and neutralized with a saturated aqueous NaHCO₃ solution. The organic layer was extracted with dichloromethane and dried

with Na_2SO_4 . The solvent was evaporated to provide a crude product, which after column chromatography on SiO_2 eluted with CH_2Cl_2 afforded green compound **10** (83.4 mg, 94% yield). ^1H NMR (300 MHz, CDCl_3): δ = 12.58 (s, 1 H, 15-CHO), 10.49 (s, 1 H, 5-H), 10.08 (d, 3J = 4.5 Hz, 1 H, 2 H, 13-H), 10.04 (d, 3J = 4.5 Hz, 2 H, 17-H), 9.31 (d, 3J = 4.8 Hz, 1 H, 7-H), 9.09 (two d, 2 H, 3J = 4.5, 12-H and 18-H), 8.93 (d, 3J = 4.5 Hz, 1 H, 8-H), 8.82 (s, 1 H, 2-H), 8.08 (m, 4 H, 2', 6' and 2'', 6''-H), 7.88 (t, 4J = 1.8 Hz, 2 H, 4', 4''-H), 6.59 (q, 3J = 6.3 Hz, 1 H, HO-CH-CH₃), 2.58 (s, 1 H, OH), 2.24 (d, 3J = 6.6 Hz, 3 H, HO-CH-CH₃), 1.56 [m, 36 H, C(CH₃)₃], -2.36 (s, 2 H, NH) ppm. UV/Vis (CH_2Cl_2): λ_{max} (nm) = 424, 525, 565, 596, 653. HR-FAB-MS: found m/z = 759.4653 [M + H]⁺, calcd. for $\text{C}_{51}\text{H}_{59}\text{N}_4\text{O}_2$ 759.4638.

rac-10,20-Bis(3,5-di-tert-butylphenyl)-15-formyl-3-(1-hydroxyethyl)-porphinatozinc (10-Zn): (Transformation **h** in the Scheme). Zinc acetate (43 mg, 0.023 mmol) was added to a solution of compound **10** (25 mg, 0.0329 mmol) in CHCl_3 (20 mL) and MeOH (12 mL), and the reaction mixture was stirred at room temp. for 3 h under inert atmosphere. The reaction mixture was then washed with brine and extracted with dichloromethane. The organic layer was dried with Na_2SO_4 and evaporated to leave the green compound **Zn-10** in high purity and yield (25.2 mg, 93.3%). ^1H NMR (300 MHz, $\text{CDCl}_3+\text{CD}_3\text{OD}$, 10:1, v/v): δ = 12.54 (s, 1 H, 15-CHO), 10.37 (s, 1 H, 5-H), 10.02 and 10.01 (two d, J = 4.9 Hz, 2 H, 13- and 17-H), 9.25 (d, J = 4.5 Hz, 1 H, 7-H), 9.05 and 9.03 (two d, J = 4.7, 4.9 Hz, 2 H, 12- and 18-H), 8.89 (d, J = 4.3 Hz, 1 H, 8-H), 8.79 (s, 1 H, 2-H), 8.01 (m, 4 H, 2', 6', 2'', 6''-H), 7.57 (t, J = 1.8 Hz, 2 H, 4', 4''-H), 6.55 (q, 3J = 6.5 Hz, 1 H, HO-CH-CH₃), 3.40 (s, 1 H, OH), 2.20 (d, J = 6.4 Hz, 3 H, HO-CH-CH₃), 1.53 [two s, 36 H, C(CH₃)₃] ppm. UV/Vis (CH_2Cl_2 + *n*-heptane): λ_{max} (nm) = 638, 594, 480, 420. After methanol addition: 607, 563, 428. UV/Vis (CH_2Cl_2 , 0.23 mM): λ_{max} (lg ϵ_{max}) = 600 (4.19), 557 (4.05), 424 (5.47). HR-FAB-MS: found m/z = 821.3782, [M + H]⁺, calcd. for $\text{C}_{51}\text{H}_{56}\text{N}_4\text{O}_2\text{Zn}$ 821.3773.

10,20-Bis(3,5-di-tert-butylphenyl)-5,15-bis(5,5-dimethyl-1,3-dioxan-2-yl)porphyrin (5): (Transformation **e** in the Scheme). A solution of 10,20-bis(3,5-di-tert-butylphenyl)-5,15-bis(formyl) porphyrin^[5] (47 mg, 0.0632 mmol), 2,2-dimethylpropanediol (100 mg; 0.99 mmol), and *p*-toluenesulfonic acid as catalyst in toluene (100 mL) was heated to reflux in a Dean-Stark apparatus for 6 h. After evaporation of the solvent, the residue was taken up in CH_2Cl_2 and washed with a saturated aqueous NaHCO_3 solution, and the solvents were evaporated off to dryness. The crude product was purified by column chromatography on SiO_2 (eluent: $\text{CH}_2\text{Cl}_2/n$ -hexane, 1:1, v/v) to leave pure **5** (43 mg; 75%) as a red solid. ^1H NMR (300 MHz, CDCl_3): 9.90 (d, 3J = 4.8 Hz, 4 H, 3,7,13,17-H), 8.94 (d, 3J = 5.1 Hz, 4 H, 2,8,12,18-H), 8.03 (d, 4J = 1.8 Hz, 4 H, Ph-ortho-H), 7.93 (s, 2 H, H_{acetal}), 7.81 (t, 4J = 1.8 Hz, 2 H, Ph-para-H), 4.31 (m, 8 H, CH₂ acetal), 1.92 (s, 3 H, CH₃-eq-acetal), 1.54 [s, 36 H, C(CH₃)₃], 1.11 (s, 3 H, CH₃-ax-acetal), -2.95 (s, 2 H, NH) ppm. UV/Vis (CHCl_3): λ_{max} (nm) = 416, 512, 544, 586, 641. HR-FAB-MS: found m/z = 915.5803, calcd. for $\text{C}_{60}\text{H}_{77}\text{N}_4\text{O}_4$ 915.5788.

10,20-Bis(3,5-di-tert-butylphenyl)-5,15-bis(5,5-dimethyl-1,3-dioxan-2-yl)chlorin (7): (Transformation **i** in the Scheme). A solution of 10,20-bis(3,5-di-tert-butylphenyl)-5,15-bis(5,5-dimethyl-1,3-dioxan-2-yl)porphyrin (**5**) (20 mg; 0.022 mmol), K_2CO_3 (90 mg; 0.65 mmol), and tosylhydrazide (40 mg, 0.215 mmol) in β -picoline (5 mL) was heated at reflux for 15 h. Water was then added, and the crude reaction mixture was extracted with CH_2Cl_2 . The organic phase was washed once with brine, twice with HCl (5%), and twice with water, and was then evaporated to dryness. The residue was purified by column chromatography on SiO_2 (eluent: $\text{CH}_2\text{Cl}_2/n$ -

hexane, 1:1, v/v) to leave pure **7** (11 mg; 55%) as a green solid. ^1H NMR (300 MHz, CDCl_3): δ = 9.75 (d, 3J = 5.1 Hz, 1 H, 3-H), 9.53 (d, 3J = 4.5 Hz, 1 H, 13-H), 9.28 (d, 3J = 4.8 Hz, 1 H, 7-H), 8.68 (d, 3J = 3.6 Hz, 1 H, 4-H), 8.51 (d, 3J = 4.5 Hz, 1 H, 8-H), 8.27 (d, 3J = 4.5 Hz, 1 H, 2-H), 7.92 (d, 4J = 1.8 Hz, 2 H, 2', 6'-H), 7.74 (t, 4J = 1.8 Hz, 1 H, 4'-H), 7.69 (t, 4J = 1.8 Hz, 1 H, 4''-H), 7.65 (d, 4J = 1.8 Hz, 2 H, 2'', 6''-H), 7.62 (s, 1 H, H_{acetal}), 7.02 (s, 1 H, H_{acetal}), 4.74 (m, 2 H, 17-CH₂), 4.20 (m, 2 H, 18-CH₂), 1.82 (s, 3 H, CH₃-eq-acetal), 1.77 (s, 3 H, CH₃-eq-acetal), 1.49 [s, 18 H, C(CH₃)₃], 1.48 [s, 18 H, C(CH₃)₃], 1.05 (s, 3 H, CH₃-ax-acetal), 1.01 (s, 3 H, CH₃-ax-acetal), -1.30 (s, 1 H, NH), -1.55 (s, 1 H, NH) ppm. UV/Vis (CHCl_3): λ_{max} (nm) = 417, 514, 541, 602, 655. HR-FAB-MS: found m/z = 945.4504 [M + H]⁺, calcd. for $\text{C}_{50}\text{H}_{57}\text{N}_4\text{O}_2$ 945.4481.

10,20-Bis(3,5-di-tert-butylphenyl)-5,15-bis(formyl)chlorin (9): (Transformation **j** in the Scheme). A solution of TiCl_4 in CHCl_3 (0.1 M, 0.5 mL, 0.05 mmol) was added dropwise by syringe, under argon, to a solution of 10,20-bis(3,5-di-tert-butylphenyl)-5,10-bis(5,5-dimethyl-1,3-dioxan-2-yl)chlorin (**6**) (30 mg; 0.032 mmol) in dry CHCl_3 (5 mL). The reaction mixture was stirred at room temperature for 15 min and then hydrolyzed by addition of a saturated aqueous NaHCO_3 solution (5 mL). The crude reaction mixture was extracted with CH_2Cl_2 , and the solvents were evaporated to dryness. Purification by column chromatography on SiO_2 (eluent: $\text{CH}_2\text{Cl}_2/n$ -hexane, 1:1, v/v) gave pure **9** (19 mg; 66%) as a green solid. ^1H NMR (300 MHz, CDCl_3): δ = 12.23 (s, 1 H, 5-CHO), 11.90 (s, 1 H, 15-CHO), 9.79 (d, 3J = 6 Hz, 1 H, 3-H), 9.57 (d, 3J = 5.1 Hz, 1 H, 13-H), 9.39 (d, 3J = 4.5 Hz, 1 H, 7-H), 8.72 (d, 3J = 5.1 Hz, 1 H, 4-H), 8.56 (d, 3J = 4.8 Hz, 1 H, 8-H), 8.35 (d, 3J = 5.1 Hz, 1 H, 2-H), 7.95 (d, 4J = 1.8 Hz, 2 H, Ph-*o*-H), 7.82 (t, 4J = 1.8 Hz, 1 H, Ph-*p*-H), 7.76 (t, 4J = 1.8 Hz, 1 H, Ph-*p*-H), 7.65 (d, 4J = 1.8 Hz, 2 H, Ph-*o*-H), 4.91 (m, 2 H, 17-CH₂), 4.23 (m, 2 H, 18-CH₂), 1.54 [s, 18 H, C(CH₃)₃], 1.51 [s, 18 H, C(CH₃)₃], -0.35 (s, 1 H, NH), -0.47 (s, 1 H, NH) ppm. UV/Vis (CHCl_3): λ_{max} (nm) = 425, 505, 531, 578, 660, 718. HR-FAB-MS: found m/z = 915.5803 [M + H]⁺, calcd. for $\text{C}_{60}\text{H}_{75}\text{N}_4\text{O}_4$ = 915.5788.

10,20-Bis(3,5-di-tert-butylphenyl)-15-formyl-5-(hydroxymethyl)chlorin (11): (Transformation **f** in the Scheme). NaBH_4 (0.9 mg; 0.024 mmol) was added to a solution of 10,20-bis(3,5-di-tert-butylphenyl)-5,15-bis(formyl)chlorin (**9**) (22 mg; 0.024 mmol) in CHCl_3 (10 mL) and MeOH (2 mL). The mixture was stirred for 30 min at room temperature, and then water (5 mL) was added. The crude reaction mixture was extracted with CH_2Cl_2 and the solvents were evaporated to dryness. Purification by column chromatography on SiO_2 (eluent: CH_2Cl_2 /hexane, 50:50) gave pure **11** (11 mg; 50%). ^1H NMR (300 MHz, CDCl_3): δ = 11.76 (s, 1 H, 15-CHO), 9.55 (d, 3J = 5.4 Hz, 1 H, 3-H), 9.17 (d, 3J = 5.1 Hz, 1 H, 13-H), 9.02 (d, 3J = 4.8 Hz, 1 H, 7-H), 8.66 (d, 3J = 4.8 Hz, 1 H, 4-H), 8.38 (d, 3J = 4.5 Hz, 1 H, 8-H), 8.12 (d, 3J = 4.8 Hz, 1 H, 2-H), 7.90 (d, 4J = 1.8 Hz, 2 H, 10-Ph-*o*-H), 7.82 (t, 4J = 1.8 Hz, 1 H, Ph-*p*-H), 7.70 (t, 4J = 1.8 Hz, 1 H, Ph-*p*-H), 7.64 (d, 4J = 1.8 Hz, 2 H, 20-Ph-*o*-H), 6.53 (d, 3J = 5.7 Hz, 2 H, CH₂OH), 4.81 (m, 2 H, 17-CH₂), 4.13 (m, 2 H, 18-CH₂), 2.40 (t, 1 H, CH₂OH), 1.50 [s, 18 H, C(CH₃)₃], 1.48 [s, 18 H, C(CH₃)₃], 0.05 (s, 1 H, NH), -0.05 (s, 1 H, NH) ppm. UV/Vis (CHCl_3): λ_{max} (nm) = 418, 516, 555, 578, 627, 681. HR-FAB-MS: found m/z = 747.4628 [M + H]⁺, calcd. for $\text{C}_{59}\text{H}_{59}\text{N}_4\text{O}_2$ 747.4638.

10,20-Bis(3,5-di-tert-butylphenyl)-15-formyl-5-(hydroxymethyl)chlorinatozinc (11-Zn): (Transformation **h** in the Scheme). $\text{Zn}(\text{OAc})_2$ (2 mg, 0.0108 mmol) was added to a solution of 10,20-bis(3,5-di-tert-butylphenyl)-15-formyl-5-(hydroxymethyl)chlorin

(11) (5 mg, 0.0054 mmol) in CHCl_3 (3 mL) and MeOH (1 mL). The mixture was stirred for 2 h at room temperature, and water (5 mL) was then added. The crude reaction mixture was extracted with CH_2Cl_2 and the solvents were evaporated to dryness. Purification by column chromatography on SiO_2 (eluent: CH_2Cl_2) gave pure **11-Zn** (5 mg; 95%). ^1H NMR (300 MHz, $\text{CDCl}_3/\text{CD}_3\text{OD}$, 10:1 v/v): δ = 11.48 (s, 1 H, 15-CHO), 9.09 (d, 3J = 4.8 Hz, 1 H, 3-H), 8.89 (d, 3J = 4.8 Hz, 1 H, 13-H), 8.74 (d, 3J = 4.5 Hz, 1 H, 7-H), 8.34 (d, 3J = 4.8 Hz, 1 H, 4-H), 8.07 (d, 3J = 4.5 Hz, 1 H, 8-H), 7.74 (d, 3J = 4.8 Hz, 1 H, 2-H), 7.73 (d, 4J = 1.8 Hz, 2 H, 10-Ph-*o*-H), 7.68 (t, 4J = 1.8 Hz, 1 H, Ph-*p*-H), 7.59 (t, 4J = 1.8 Hz, 1 H, Ph-*p*-H), 7.49 (d, 4J = 1.8 Hz, 2 H, 20-Ph-*o*-H), 6.26 (d, 3J = 5.7 Hz, 2 H, CH_2OH), 4.66 (m, 2 H, 17- CH_2), 4.04 (m, 2 H, 18- CH_2), 1.48 [s, 18 H, $\text{C}(\text{CH}_3)_3$], 1.42 [s, 18 H, $\text{C}(\text{CH}_3)_3$] ppm. UV/Vis (CHCl_3 + MeOH): λ_{max} (nm) = 419, 639. UV/Vis (CH_2Cl_2 + MeOH, 0.13 mM): λ_{max} (lg ϵ_{max}) = 642 (4.16), 599 (3.77), 522 (3.51), 421 (5.01). HR-FAB-MS: found m/z = 809.3760 $[\text{M} + \text{H}]^+$, calcd. for $\text{C}_{50}\text{H}_{57}\text{N}_4\text{O}_2\text{Zn}$ 809.3772.

Acknowledgments

Professor Nils Metzler-Nolte is thanked for enabling us to record the CD spectra. Professor Hitoshi Tamiaki kindly shared unpublished results^[31] and enriching discussions with us. Matthias Fischer is thanked for technical assistance, and Ingrid Roßnagel for HR-FAB-MS measurements. This work was partially financed by the DFG-Center for Functional Nanostructures at the University of Karlsruhe, through project C3.2.

- [1] [1a] T. S. Balaban, A. R. Holzwarth, K. Schaffner, G.-J. Boender, H. J. M. de Groot, *Biochemistry* **1995**, *34*, 15259. [1b] B. J. van Rossum, D. B. Steensgaard, F. M. Mulder, G. J. Boender, K. Schaffner, A. R. Holzwarth, H. J. M. de Groot, *Biochemistry* **2001**, *40*, 1587.
- [2] [2a] R. E. Blankenship, J. M. Olson, M. Miller, "Antenna complexes from green photosynthetic bacteria" in *Anoxygenic photosynthetic bacteria* (Eds.: R. E. Blankenship, M. T. Madigan, C. E. Bauer), Kluwer Academic, **1995**; pp. 399–435. [2b] R. E. Blankenship, *Molecular Mechanisms of Photosynthesis*, Blackwell Science, Oxford, **2002**. [2c] T. S. Balaban, "Light-harvesting nanostructures" in *Encyclopedia of Nanoscience and Nanotechnology* (Ed.: H. S. Nalwa), American Scientific Publishers, Los Angeles, **2004**, vol. 4, pp. 505–559.
- [3] [3a] T. S. Balaban, A. R. Holzwarth, K. Schaffner, *J. Mol. Struct.* **1995**, *349*, 183. [3b] J. Chiefari, K. Griebenow, F. Fages, N. Griebenow, T. S. Balaban, A. R. Holzwarth, K. Schaffner, *J. Phys. Chem.* **1995**, *99*, 1357. [3c] T. S. Balaban, H. Tamiaki, A. R. Holzwarth, K. Schaffner, *J. Phys. Chem.* **1997**, *101*, 3424. [3d] T. S. Balaban, J. Leitich, A. R. Holzwarth, K. Schaffner, *J. Phys. Chem. B* **2000**, *104*, 1362.
- [4] [4a] P. Cheng, P. A. Liddell, S. X. C. Ma, R. E. Blankenship, *Photochem. Photobiol.* **1993**, *58*, 290. [4b] T. Mizoguchi, L. Limantara, K. Matsuura, K. Shimada, Y. Koyama, *J. Mol. Struct.* **1996**, *379*, 249. [4c] Z.-Y. Wang, M. Umetsu, K. Yoza, M. Kobayashi, M. Imai, Y. Matsushita, N. Niimura, T. Nozawa, *Biochim. Biophys. Acta* **1997**, *1320*, 73. [4d] Z.-Y. Wang, M. Umetsu, M. Kobayashi, T. Nozawa, *J. Am. Chem. Soc.* **1999**, *121*, 9363. [4e] Z.-Y. Wang, M. Umetsu, M. Kobayashi, T. Nozawa, *J. Phys. Chem. B* **1999**, *103*, 3742. [4f] T. Mizoguchi, K. Ogura, F. Inagaki, Y. Koyama, *Biospectroscopy* **1999**, *5*, 63.
- [5] T. S. Balaban, A. D. Bhise, M. Fischer, M. Linke-Schaetzel, C. Roussel, N. Vanthuyne, *Angew. Chem. Int. Ed.* **2003**, *42*, 2140; *Angew. Chem.* **2003**, *115*, 2189.
- [6] M. Linke-Schaetzel, A. D. Bhise, H. Gliemann, T. Koch, T. Schimmel, T. S. Balaban, *Thin Solid Films* **2004**, *451/452*, 16–21.
- [7] [7a] S. Yagai, H. Miyatake, H. Tamiaki, *J. Org. Chem.* **2002**, *67*, 49. [7b] For a review of earlier work on semisynthetic BChl *c* mimics see: H. Tamiaki, *Coord. Chem. Rev.* **1996**, *148*, 183. [7c] H. Tamiaki, T. Miyatake, R. Tanikaga, A. R. Holzwarth, K. Schaffner, *Angew. Chem. Int. Ed. Engl.* **1996**, *35*, 772; *Angew. Chem.* **1996**, *108*, 810. [7d] T. Miyatake, T. Oba, H. Tamiaki, *Chem. Bio. Chem.* **2001**, 335.
- [8] H. Tamiaki, S. Kimura, T. Kimura, *Tetrahedron* **2003**, *59*, 7423.
- [9] T. S. Balaban, J.-M. Lehn, S. Lebedkin, M.-J. Brienne, *Ger. Offen.* **2003**, Patent DE 101 46 970 A1.
- [10] K. Susumu, T. Shimidzu, K. Tanaka, H. Segawa, *Tetrahedron Lett.* **1996**, *37*, 8399.
- [11] [11a] M. J. Crossley, P. L. Burn, *J. Chem. Soc., Chem. Commun.* **1987**, 39. [11b] M. J. Crossley, P. L. Burn, *J. Chem. Soc., Chem. Commun.* **1991**, 1569. [11c] We propose to nickname the 3,5-di-*tert*-butylphenyl substituent "Crossley's crutch", as it helps porphyrin chemists in four ways: (i) it solubilizes complex architectures and minimizes π -stacking of *meso*-aryl porphyrins, thanks to its steric bulge, (ii) it prevents electrophilic substitution in the adjacent β -pyrrolic positions and on the benzene ring, thus enabling very selective functionalization of the porphyrins, (iii) it packs well into crystals, enabling X-ray diffraction studies to be carried out^[12,24] but at the same time enables visualization by scanning probe techniques^[34] for noncrystalline samples, and (iv) thanks to the sharp NMR *tert*-butyl singlet, visible even in nanomolar concentrations, it allows easy identification of compounds and of their symmetry in order to allow monitoring of complex reaction mixtures.
- [12] T. S. Balaban, R. Goddard, M. Linke-Schaetzel, J.-M. Lehn, *J. Am. Chem. Soc.* **2003**, *125*, 4233.
- [13] J.-M. Lehn, *Supramolecular Chemistry: Concepts and Perspectives*, VCH Verlagsgesellschaft, Weinheim, **1995**.
- [14] A. Kay, M. Grätzel, *J. Phys. Chem.* **1993**, *97*, 6272.
- [15] J.-P. Strachan, D. F. O'Shea, T. Balasubramanian, J. S. Lindsey, *J. Org. Chem.* **2000**, *65*, 3160.
- [16] [16a] D. T. Gryko, C. Clausen, J. S. Lindsey, *J. Org. Chem.* **1999**, *64*, 8635. [16b] A. Osuka, G. Noya, S. Taniguchi, T. Okada, Y. Nishimura, I. Yamazaki, N. Mataga, *Chem. Eur. J.* **2000**, *6*, 33.
- [17] [17a] H. W. Whitlock Jr., R. Hanauer, M. Y. Oester, B. K. Bower, *J. Am. Chem. Soc.* **1969**, *91*, 7485. [17b] M. O. Senge, W. W. Kalish, S. Runge, *Tetrahedron* **1998**, *54*, 3781. [17c] M. Pineiro, A. L. Carvalho, M. M. Pereira, A. M. d'A. Rocha Gonsalves, L. G. Arnaut, S. J. Formosinho, *Chem. Eur. J.* **1998**, *4*, 2299. [17d] Y. Ferrand, L. Bourre, G. Simonneaux, S. Thibaut, F. Odobel, Y. Lajat, T. Patrice, *Bioorg. Med. Chem. Lett.* **2003**, *13*, 833. [17e] J. Laville, T. Figueiredo, B. Loock, S. Pigaglio, R. Maillard, D. S. Grierson, D. Carrez, A. Croisy, J. Blais, *Bioorg. Med. Chem.* **2003**, *11*, 1643.
- [18] An analogy to the (bacterio)chlorophyll numbering is preserved here. Confusion may arise due to systematic nomenclature, which places a hydroxy(m)ethyl group after formyl, thus reversing the numbering sense of the macrocycle between the different compounds in the Scheme.
- [19] Not only the color, but also the shift of the $\tilde{\nu}_{\text{C=O}}$ frequencies give strong indications of whether an acyl substituent has the carbonyl group in conjugation with the macrocycle (A. D. Bhise, M. Linke-Schaetzel, D. Moss, T. S. Balaban, manuscript in preparation).
- [20] [20a] G. McDermott, S. M. Prince, A. A. Freer, A. Hawthornthwaite-Lawless, M. Z. Papiz, R. J. Cogdell, N. W. Isaacs, *Nature* **1995**, *374*, 517. [20b] J. Koepke, X. Hu, C. Muenke, K. Schulten, H. Michel, *Structure* **1996**, *4*, 581.
- [21] K. McLuskey, S. M. Prince, R. J. Cogdell, N. Isaacs, *Biochemistry* **2001**, *40*, 8783.
- [22] [22a] L. Dähne, *J. Am. Chem. Soc.* **1995**, *117*, 12855. [22b] M. Wang, G. L. Silva, B. A. Armitage, *J. Am. Chem. Soc.* **2000**, *122*, 9977. [22c] C. Thalacker, F. Würthner, *Adv. Funct. Mater.* **2002**, *12*, 209. [22d] A. P. H. J. Schenning, J. v. Herrikhuyzen, P. Jonkheijm, Z. Chen, F. Würthner, E. W. Meijer, *J. Am. Chem. Soc.* **2002**, *124*, 10252. [22e] H. von Berlepsch, S. Kirstein, R.

- Hania, C. Didraga, A. Pugžlys, C. Böttcher, *J. Phys. Chem. B* **2003**, *107*, 14176; for reviews see: ^[22f] D. Möbius, *Adv. Mater.* **1995**, *7*, 437. ^[22g] A. Mishra, R. K. Behera, P. K. Behera, B. K. Mishra, G. M. Behera, *Chem. Rev.* **2000**, *100*, 1973.
- ^[23] HyperChem[®], Hypercube Inc. Release 7, Gainesville, Florida, **2002**.
- ^[24] ^[24a] T. S. Balaban et al. unpublished results. ^[24b] T. S. Balaban, M. Linke-Schaetzel, A. D. Bhise, N. Vanthuyne, C. Roussel, C. E. Anson, G. Buth, A. Eichhöfer, K. Foster, G. Garab, H. Gliemann, R. Goddard, T. Javorfi, A. K. Powell, H. Rösner, Th. Schimmel, submitted for publication.
- ^[25] M. Umetsu, Z.-Y. Wang, M. Kobayashi, T. Nozawa, *Biochim. Biophys. Acta* **1999**, *1410*, 19.
- ^[26] ^[26a] K. M. Smith, G. M. F. Bisset, M. Bushell, *J. Org. Chem.* **1980**, *45*, 2218. ^[26b] B. Gerlach, S. E. Brantley, K. M. Smith, *J. Org. Chem.* **1998**, *63*, 2314.
- ^[27] ^[27a] D. Keller, C. Bustamante, *J. Chem. Phys.* **1986**, *84*, 2972. ^[27b] M.-H. Kim, L. Ulibarri, D. Keller, M. F. Maestre, C. Bustamante, *J. Chem. Phys.* **1986**, *84*, 2981.
- ^[28] ^[28a] N. Berova, K. Nakanishi, in *Circular Dichroism. Principles and Applications, 2nd ed* (Eds.: N. Berova, K. Nakanishi, R. W. Woody), John Wiley & Sons, New York, **2000**, pp. 337–382.
- ^[28b] G. Pescitelli, S. Gabriel, Y. Wang, J. Fleischhauer, R. W. Woody, N. Berova, *J. Am. Chem. Soc.* **2003**, *125*, 7613.
- ^[29] V. I. Prokhorenko, D. B. Steensgard, A. R. Holzwarth, *Biophys. J.* **2003**, *85*, 3173.
- ^[30] C. Didraga, J. A. Klugkist, J. Knoester, *J. Phys. Chem. B* **2002**, *106*, 11474.
- ^[31] ^[31a] H. Kitamoto, Master Thesis **2002**, Ritsumeikan University, Kusatsu, Shiga, Japan. ^[31b] H. Tamiaki, H. Kitamoto, T. Watanabe, R. Shibata, submitted for publication. ^[31c] H. Tamiaki, H. Kitamoto, A. Nishikawa, T. Hibino, R. Shibata, *Bioorg. Med. Chem.* **2004**, *12*, 1657.
- ^[32] For a review on organic solar cells see: C. J. Brabec, N. S. Sariciftci, J. C. Hummelen, *Adv. Funct. Mater.* **2001**, *11*, 15.
- ^[33] ^[33a] C. Roussel, J. Pierrot-Sanders, I. Heitmann, P. Piras, in *Chiral Separation Techniques – A Practical Approach*, G. Subramanian (Ed.), Wiley-VCH, Weinheim, **2001**. ^[33b] The data can be obtained free of charge upon request mentioning the article's reference at: CHIRBASE Project, Case A-62, University Aix-Marseille III, 13397 Marseille, Cedex 20, France.
- ^[34] ^[34a] T. A. Jung, R. R. Schlittler, J. K. Gimzewski, *Nature* **1997**, *386*, 696. ^[34b] J. K. Gimzewski, C. Joachim, *Science* **1999**, *283*, 1683.

Received March 8, 2004